Geoderma 442 (2024) 116787

Contents lists available at ScienceDirect

Geoderma

journal homepage: www.elsevier.com/locate/geoderma

Rewetting drained peatlands through subsoil infiltration stabilises redox-dependent soil carbon and nutrient dynamics

Sarah F. Harpenslager [a,b,*], Gijs van Dijk [a,b], Jim Boonman [c], Stefan T.J. Weideveld [a,b], Bas P. van de Riet [a,b], Mariet M. Hefting [d,e], Alfons J.P. Smolders [a,b]

[a] B-WARE Research Centre, Toernooiveld 1, 6525 ED Nijmegen, the Netherlands
[b] Department of Aquatic Ecology and Environmental Biology, Radboud Institute of Biological and Environmental Sciences, Radboud University, Heyendaalseweg 135, 6525 AJ Nijmegen, the Netherlands
[c] Faculty of Science, Department of Earth Sciences, Vrije Universiteit Amsterdam, Amsterdam 1081 HV, the Netherlands
[d] (Amsterdam Institute of Life Science and Environment) A-LIFE Section Systems Ecology, Vrije Universiteit Amsterdam, Amsterdam 1081 HV, the Netherlands
[e] Department of Biology, Institute of Environmental Biology, Utrecht University, Utrecht 3508 TB, the Netherlands

ARTICLE INFO

Handling Editor: M. Tighe

Keywords:
Biogeochemistry
Rewetting
Peat meadows
Agricultural use
Groundwater levels
Applied research

ABSTRACT

Centuries of drainage have stimulated peat decomposition. To counteract the resulting increase in greenhouse gas emission and land subsidence in Dutch agricultural peatlands, passive and active subsurface infiltration (SSI) systems have been developed for peatland rewetting. Here, we studied the effects of SSI systems on groundwater levels, porewater composition and redox potential in four drained peatlands in the Netherlands to determine how soil processes are affected, especially carbon and nutrient dynamics. For three years, groundwater levels were measured continuously, and porewater samples were collected 8–10 times per year in paired SSI (active and passive) and control plots. SSI plots had higher summer groundwater levels and less seasonal fluctuation in groundwater levels than control plots. Redox potential and porewater composition in control plots reflected dominance of oxidation processes during dry periods in the upper soil layers, whereas SSI plots showed dominance of reduction processes in these layers throughout the year. These differences between control and SSI plots were strongest at locations with active SSI systems. Our results show that SSI systems can be effective measures to raise and stabilise groundwater levels in drained peatlands, which results in more stable redox zonation and dominance of anaerobic soil processes, especially during dry periods and when active SSI systems are applied. On the short term, a switch from oxic to anoxic conditions can cause mobilisation of phosphorus and ammonium, while on the longer term the application of SSI can lead to substantial change in carbon and nutrient dynamics. Understanding the full effects of implementing SSI systems and other mitigation measures in drained peatlands is important before they are applied on a large scale.

1. Introduction

Since the 12th and 13th centuries, lowland peat areas have been drained to support agricultural use. Worldwide, about 15 % of peatlands have been drained for agriculture, forestry and other human activity during the 20th century (Joosten et al., 2016; Ziegler et al., 2021). Drainage enhances the aerobic decomposition of peat, turning former carbon (C) sinks into C sources (Leifeld et al., 2019). Dutch drained peatlands emit an estimated 4.3 Mt of CO_2-eq each year, which is approximately 2–3 % of the total national greenhouse gas emission (Arets et al., 2021). Additionally, both peat oxidation and consolidation have led to cumulative land subsidence of 2–4 m since the Middle Ages (Erkens et al., 2016; van Asselen et al., 2018), thereby necessitating further drainage to keep the land suitable for agriculture. Despite continued drainage, lowland peat areas in the Netherlands remain too wet to support arable crop production and approx. 80 % of Dutch peatlands are therefore currently used as production grassland and dairy farms (Tanneberger et al., 2017; Van den Born et al., 2016).

Drained peatlands experience strong fluctuations in GWLs, with higher water levels in winter and much lower water levels in summer, resulting in a peat layer that is seasonally oxidised and reduced. Consequently, these soil layers have become rich in iron and

* Corresponding author.
E-mail addresses: E-mail address: s.f.harpenslager@b-ware.eu (S.F. Harpenslager). sarahfaye.harpenslager@ru.nl (S.F. Harpenslager).

https://doi.org/10.1016/j.geoderma.2024.116787
Received 3 August 2023; Received in revised form 12 January 2024; Accepted 16 January 2024
Available online 25 January 2024

phosphorus, while nitrogen and sulphates wash out to deeper soil layers, groundwater or the surrounding surface water (Smolders et al., 2010; van Diggelen et al., 2020). Leaching of solutes (e.g. nutrients, dissolved (in)organic carbon and sulphate) from fertilised peat soils can have a large impact on the quality of the surrounding surface water in agricultural peatlands (van Beek et al., 2007; Vermaat and Hellmann, 2010).

To counteract both land subsidence and greenhouse gas emissions from agricultural lowland peat areas, different mitigation measures are being taken to reduce peat oxidation, including controlling water levels in surrounding ditches, infiltration through shallow trenches on pastures and installing sub-surface infiltration (SSI) systems (Hoving et al., 2020). These measures are all aimed at reducing groundwater level (GWL) fluctuations and raising GWLs in summers. SSI systems consist of drains that are installed at least 10 cm below targeted ditch water level to passively irrigate drained peatlands with surface water in times of drought (Querner et al., 2012), thereby reducing GWL fluctuations (Best and Jacobs, 1997; Kechavarzi et al., 2007). By infiltrating water directly into the soil, SSI systems tackle some of the efficiency problems experienced by other mitigation measures (including raising ditch water levels) due to the low hydraulic conductivity and lateral flow in the unsaturated zone of peat soils. Since the Netherlands has a net precipitation surplus of approximately 300 mm per year (KNMI, 2023), SSI systems also function as traditional drainage systems during wet periods, which may allow agricultural activities earlier in the year (i.e. supporting cattle and heavy machinery). Newer SSI systems consist of pressurised systems, where a pump is used to maintain a target water level in a buffer compartment between parcel and surface water (Hoekstra et al., 2020). This allows for more active control of the GWLs and creates extra pressure to promote the lateral waterflow in peat soils.

Application of SSI systems generally raises and stabilises GWLs (Boonman et al., 2022; Hoekstra et al., 2020; Weideveld et al., 2021). These systems are installed to counteract peat decomposition, soil subsidence and greenhouse gas emission, although recent studies have shown inconsistent results on their efficiency in reducing greenhouse gas emission (Boonman et al., 2022; Weideveld et al., 2021). Altering GWL dynamics in peatlands that have been subjected to drainage for hundreds of years would, however, have a profound effect on soil redox conditions and biogeochemical processes that may be obscured in direct greenhouse gas emission measurements. Raising GWLs through SSI systems changes the depth of oxygen intrusion into the soil (Estop-Aragonés et al., 2012) and the dominance of anaerobic processes using alternative electron acceptors such as nitrate (NO_3^-), ferric iron (Fe^{3+}) and sulphate (SO_4^{2-}) in shallower soil layers (de Jong et al., 2020; Dean et al., 2018). Anaerobic peat decomposition with alternative electron acceptors generally proceeds at a slower rate than aerobic peat decomposition (Bridgham et al., 1998; Updegraff et al., 1995), depending on organic matter quality and electron acceptor availability. Especially in the first period after rewetting, reduction of oxidised soil complexes (such as iron(hydr)oxides) can still have strong effects on the nutrient availability and emission of greenhouse gasses (CH_4 and N_2O) in organic soils. Although studies exist where these effects of rewetting degraded peat soils have been simulated in laboratory incubations of soil cores with different water levels (Harpenslager et al., 2015; Van de Riet et al., 2013), large-scaled field studies are scarce. It is, however, important to understand how mitigation measures affect not only greenhouse gas emission and land subsidence, but also biogeochemical soil processes and nutrient mobilisation before such measures are applied on a large scale. In addition, it is unclear if there are strong differences between the effects of passive and active SSI systems on biogeochemical soil processes.

Here, we present three years of biogeochemical data that were collected in four drained peatlands with active dairy farming in the western and northern parts of the Netherlands. Using temporal and spatial porewater and redox dynamics as a proxy for dominant biogeochemical processes, we determined the effects of two different SSI systems (active and passive) on soil processes, focusing on soil nutrient and carbon dynamics. Since SSI systems are applied to reduce GWL drops and fluctuations, we expect more stable redox zonation and fewer, shorter and shallower occurrences of aerobic oxidation processes on SSI plots than in control plots. We further expect that pressurised, active SSI systems are more effective in raising GWLs and stabilising biogeochemical soil processes than passive SSI systems, and that these effects can be observed throughout the parcel while they may be more localised around the SSI system in parcels with passive SSI systems. Efficiency of SSI systems may also depend on site-specific conditions, including soil build-up and land use history. Given the typical iron-rich and nutrient-rich topsoils of Dutch drained agricultural peatlands, we expect mobilisation of iron, phosphorus and ammonium as a result of reduction processes due to increased GWLs. By gaining insight into the effects of mitigation measures such as SSI systems on soil biogeochemical processes, the large-scale implementation of such measures can be evaluated and optimised.

2. Methods

2.1. Site descriptions

Four locations – Assendelft (ASD), Zegveld (ZEG), Aldeboarn (ALB) and Vlist (VLI) - were selected in the western and northern part of the Netherlands (Fig. 1). All sites are situated within typical Dutch coastal peatland areas and have been influenced by drainage and agricultural activity for hundreds of years. Reclamation of coastal peatlands started from 800 CE onwards with larger-scaled reclamation from the 12th or 13th century. In the beginning, peatlands were used to grow arable crops (such as grain or hemp) but over time land subsidence led to wetter conditions, which limited crop production. From the 15th century onwards, active drainage by wind mills was used to create suitable conditions for pastures and dairy farming (Borger, 1992). The combined effect of large groundwater fluctuations and, from the 1930s onwards, high nutrient input created an oxidised top layer (~30–50 cm) with high iron and phosphorus contents on these agriculturally used peatlands (Table 1). The peat in the study sites shows degraded and amorphous peat in the topsoil with a higher content of mineral particles and consequently a lower organic matter content and higher bulk-density in the upper soil layers compared to deeper, more intact peat layers that remain water saturated. In ZEG and VLI, this peat mainly consists of wood peat, while ASD is characterised by eutrophic reed-sedge peat and ALB by oligotrophic peat consisting of *Sphagnum* moss, *Eriophorum* and heather (Table 1). Western locations, especially ASD, had a higher total-S content than the northern site of ALB (Table 1). Out of the four locations, ALB had the lowest total P-content and lower availability of NO_3^- and NH_4^+ (Table 1).

2.2. Experimental set-up

At each location, a monitoring plot was created on a parcel with and on a parcel without sub-soil infiltration systems (Fig. 1). Two locations, Assendelft (ASD; installed 2017) and Zegveld (ZEG; installed 2016), had pressurized, active SSI systems, whereas the other two locations, Aldeboarn (ALB; installed 2016) and Vlist (VLI; installed 2011) had regular, passive SSI systems. In the sites with active SSI systems, automated target groundwater levels (GWL) were set to 26 and 35 cm below ground level for ASD and ZEG, respectively. The rectangular experimental plots measured approximately 200–250 m^2. On parcels with SSI, drains were present at a depth of ~70 cm with 6 m spacing between drains, except in ASD, where drains had been installed at 50 cm below ground level with 4 m spacing. Ceramic cups (pore size 0.45 μm) for porewater collection were installed at 45–50, 75–80 and 120–125 cm below ground level. Sampling depths were chosen to reflect soil layers that were always above mean summer GWL (45–50 cm), soil layers that were only above mean summer GWL during drought (75–80 cm) and soil layers that were permanently water saturated (120–125 cm). Groundwater level loggers

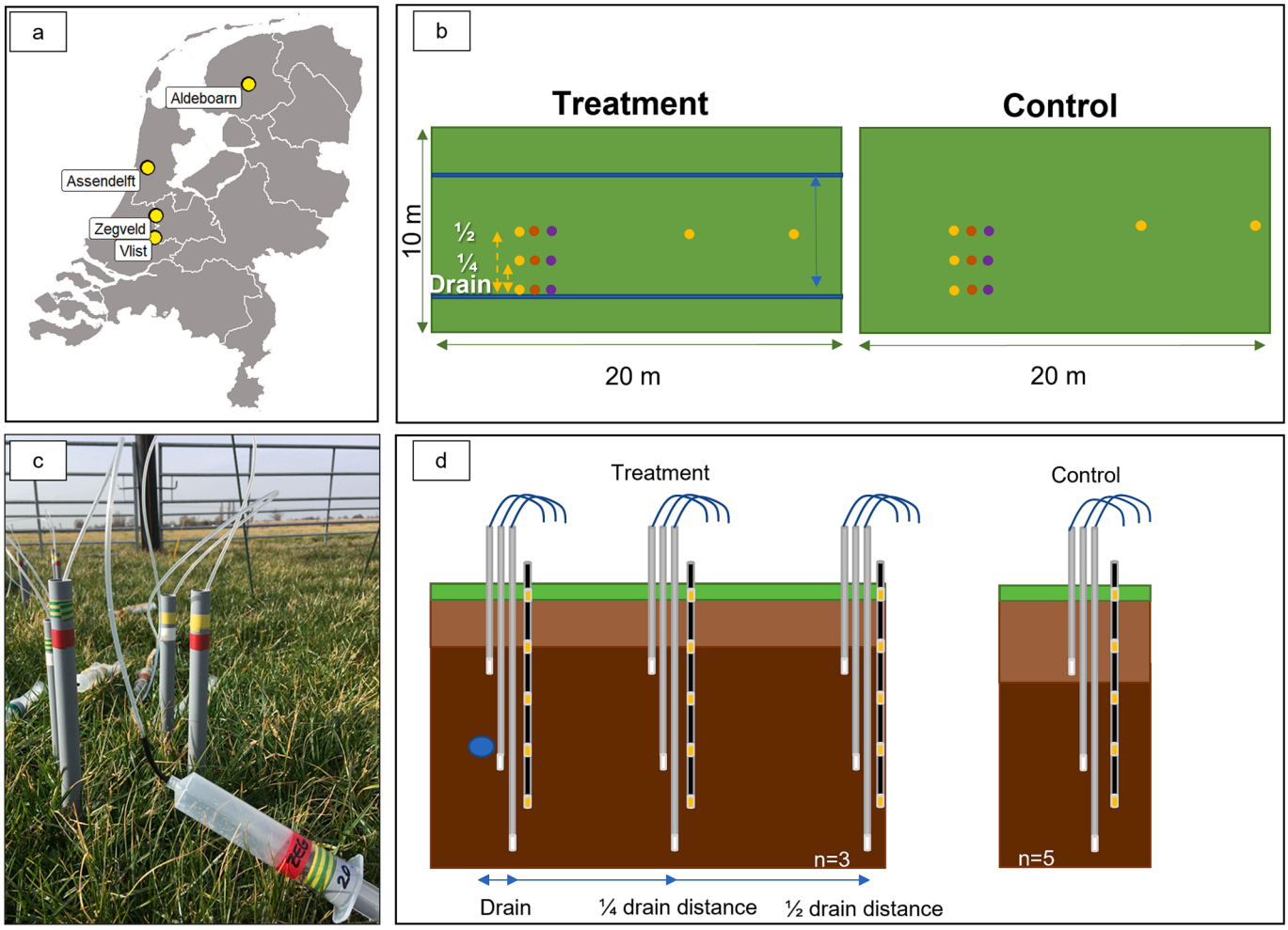

Fig. 1. Experimental set-up, with an overview of (a) the location of the four study sites and (b) the experimental plots with (left) and without (right) SSI systems. Drain distance was 6 m in all sites, apart from Assendelft, where drains were 4 m apart. Porewater sampling, redox loggers and GWL loggers are indicated by yellow, orange and purple dots, respectively. Porewater was collected using vacuum syringes attached to ceramic cups (c), which were fixed at 45, 75 and 120 cm below ground level (d). Redox potential was measured at 10, 30, 50, 70 and 90 cm depth (indicated by yellow-black rods). In the SSI plot (1d left), ceramic cups and redox sensors were placed along a gradient from the SSI inlet (blue circle).

(Ellitrack, Leiderdorp Instruments, Leiderdorp, The Netherlands) were installed inside monitoring wells with a filter depth from 0.3–1.3 m (ASD), 0.3–1.5 m (ZEG), 0.75–1.70 m (ALB) and 0.5–1.5 m (VLI), to record hourly GWLs. More detailed analyses of GWLs in these study locations can be found in van Asselen et al., 2023. Redox probes (previously described in Vorenhout et al., 2011), consisting of platinum electrodes (Paleo Terra, Oijen, The Netherlands) installed at 10, 30, 50, 70 and 90 cm depth and a KCl reference electrode (209 mV at 15 °C), were connected to Campbell CR-1000X data loggers (Campbell Scientific, Logan, UT, USA). In plots with SSI systems, ceramic cups were installed at the drain (n = 1), at ¼ drain distance (n = 1) and at ½ drain distance (n = 3; to include spatial variation within the plot). Additionally, one GWL logger and one redox probe were installed at each drain distance. In control plots, ceramic cups (n = 5), GWL loggers (n = 3) and redox probes (n = 3) were installed according to the same spatial distribution as in the infiltrated plot (Fig. 1). Since all experimental plots were on active farms, they were typically fertilised five times per year and mown five to nine times per year. The dominant species was perennial ryegrass (*Lolium perenne*).

2.3. Sample collection

Porewater samples were collected between April 2020 and March 2023, with monthly sampling during the growing season (April to September) and two to four sampling events outside the growing season (October to March). At the two locations with active SSI (Assendelft and Zegveld), sampling frequency was increased bi-monthly between April and September 2021 and 2022. Porewater was collected by attaching 60 mL syringes to ceramic cups with gastight tubing and manually creating a vacuum. After collection of the syringes, additional porewater was sampled to determine dissolved methane and sulphide concentrations by attaching a hypodermic needle to the gastight tube and connecting a 12 mL pre-vacuumed gastight vial (containing 1 mL 0.5 M HCl to halt microbial activity; Labco, Lampeter, UK). Vials were kept upside down to reduce risk of gas leakage. All samples were kept cool during transport to the laboratory for analyses the next day.

Soil cores were collected next to each ceramic cup between 28 June and 6 July 2021. Samples were collected from 0 to 10 cm, 20–30 cm, 40–50 cm, 70–80 cm and 120–130 cm below ground level, thus including the depths at which porewater was collected. Samples were carefully wrapped in plastic to limit influence of atmospheric oxygen during transport.

2.4. Soil analyses

Soil profiles were visually inspected to identify the different soil layers and the soil composition was determined to characterise the different study sites (see Table 1). At the laboratory, fresh soil was

Table 1
Soil profile description, historical land-use, drainage depth and soil characteristics at each of the study locations, including organic matter (OM) fraction, bulk density (BD in kg dry soil per L fresh soil) and soil contents of total-Fe, total-S, total-P, NO_3^- and NH_4^+. Means are given ± standard deviation (n = 5). Total Fe, total-S and total-P are given in mmol per kg dry soil, whereas NO_3^- and NH_4^+ are given in μmol per kg dry soil. Locations are ASD (Assendelft, north-west), ZEG (Zegveld, west), ALB (Aldeboarn, north) and VLI (Vlist, west).

Site	Depth	Peat type	Soil build-up	Ditch drainage depth (cm)	Historical land-use	OM fraction	BD (kg L^{-1})	Total-Fe (mmol kg DW^{-1})	Total-S (mmol kg DW^{-1})	Total-P (mmol kg DW^{-1})	NO_3^- (μmol kg DW^{-1})	NH_4^+ (μmol kg DW^{-1})
ASD	0–10	Eutrophic reed-sedge peat	2 m peat on top of 13 m marine clayey and sandy deposits	45	Pasture on drained peatland	0.39 ± 0.03	0.50 ± 0.04	352 ± 69	102 ± 14	72.8 ± 12.6	1427 ± 985	56 ± 58
	20–30					0.36 ± 0.07	0.53 ± 0.07	440 ± 106	126 ± 51	51.2 ± 16.1	1313 ± 662	46 ± 45
	40–50					0.65 ± 0.16	0.27 ± 0.11	178 ± 57	405 ± 166	25.4 ± 10.3	1547 ± 1346	483 ± 555
	70–80					0.83 ± 0.04	0.12 ± 0.01	189 ± 58	1077 ± 80	9.8 ± 0.8	80 ± 159	2698 ± 1032
	120–130					0.89 ± 0.01	0.09 ± 0.02	203 ± 44	938 ± 60	8.6 ± 0.6	12 ± 6	6441 ± 1123
ZEG	0–10	Wood peat	0.2–0.5 m clayey, amorphous peat, 0–3 m wood peat, 3–5 m eutrophic reed-sedge peat, 5–5.1 clay, 5.1–9 m peat (Cladium mariscus and wood)	55	Pasture on drained peatland	0.43 ± 0.06	0.39 ± 0.03	329 ± 64	140 ± 37	73.6 ± 6.9	4555 ± 2386	291 ± 109
	20–30					0.47 ± 0.12	0.34 ± 0.07	394 ± 54	178 ± 75	41.0 ± 5.9	2226 ± 548	167 ± 92
	40–50					0.69 ± 0.06	0.23 ± 0.04	270 ± 36	360 ± 59	23.1 ± 5.7	1415 ± 636	389 ± 452
	70–80					0.76 ± 0.07	0.17 ± 0.02	221 ± 47	747 ± 139	13.2 ± 6.0	359 ± 561	2667 ± 1909
	120–130					0.8 ± 0.03	0.14 ± 0.02	165 ± 38	825 ± 79	8.6 ± 1.0	61 ± 17	6136 ± 1296
ALB	0–10	Oligotrophic peat, Spaghnum mosses, Eriophorum and heather	0.25–0.65 m clay; <0.95 m decomposed peat; <2 m oligotrophic peat; <7–8 m Pleistocene sand	70–80 (45 cm during drought)*	Pasture on drained peatland	0.2 ± 0.02	0.69 ± 0.07	400 ± 40	44 ± 7	53.5 ± 9.5	879 ± 343	324 ± 490
	20–30					0.21 ± 0.14	0.71 ± 0.15	432 ± 99	71 ± 94	40.7 ± 12.8	501 ± 242	413 ± 908
	40–50					0.56 ± 0.25	0.34 ± 0.16	265 ± 111	247 ± 126	22.5 ± 10.3	887 ± 63	375 ± 411
	70–80					0.96 ± 0.01	0.12 ± 0.0	42 ± 19	399 ± 41	4.2 ± 0.7	68 ± 106	501 ± 679
	120–130					0.89 ± 0.24	0.17 ± 0.18	64 ± 124	297 ± 97	7.3 ± 13.2	118 ± 237	2017 ± 1094
VLI	0–10	Wood peat	0–0.4 m humic clay, 0.4–2 wood peat, 2–2.3 clay, 2.3–10 m eutrophic (sedge, reed and/or wood) peat alternating with clay layers	45 in summer, 55 in winter	Pasture on drained peatland	0.45 ± 0.03	0.50 ± 0.00	405 ± 36	145 ± 10	71.0 ± 4.1	2490 ± 1023	522 ± 614
	20–30					0.2 ± 0.02	0.83 ± 0.06	712 ± 62	56 ± 7	25.6 ± 1.3	766 ± 150	83 ± 49
	40–50					0.54 ± 0.14	0.22 ± 0.02	298 ± 100	297 ± 96	21.4 ± 2.3	1119 ± 309	181 ± 98
	70–80					0.76 ± 0.02	0.17 ± 0.0	267 ± 67	840 ± 139	9.7 ± 1.3	279 ± 268	1375 ± 593
	120–130					0.78 ± 0.05	0.15 ± 0.00	156 ± 90	773 ± 170	8.2 ± 1.6	77 ± 13	8632 ± 2550

* Drainage depth was raised in ALB to 45 cm in the summer of 2020. In 2022, the water management was changed to "high if possible, low if necessary", which means that the water level is set high (ca. 45 cm below ground level) during dry periods and low (70–80 cm below ground level) if necessary for agricultural practice.

weighed into a tin cup (exactly 40.5 mL), dried at 60 °C for > 48 hrs (until stable weight) and weighed again to determine the bulk density. Organic matter content was subsequently determined by re-weighing after loss on ignition (4 hrs at 550 °C). The carbon (C) and nitrogen (N) content was determined by exactly weighing 10–35 mg of homogenised dried soil into tin cups (amount depending on the organic C content) and re-weighing after combustion at 1020 °C in a CNS elemental analyser (Vario Micro Cube, Elementar, Langenselbold, Germany). Total phosphorus (P), iron (Fe) and sulphur (S) content was determined by digesting 200 mg of homogenised soil with 5 mL 65 % HNO_3 and 2 mL 30 mL H_2O_2 in a microwave (Ethos Easy, Milestone, Sorisole, Italy). Samples were subsequently filled to 100 mL with demineralised water and analysed using inductively coupled spectrometry (axial plasma observation, seaspray nebulizer, 1300 W, 12 L/min coolant flow; ICP-OES ARCOS MV, Spectro Analytical Instruments, Kleve, Germany). Soil extractable inorganic nitrogen was determined by incubating 17.5 g of fresh soil with 50 mL of 0.2 M NaCl for 2 hrs (at 105 rpm on an orbital shaker). After determining the pH using a standard $Ag/AgCl_2$ electrode connected to a Radiometer (Type TIM840, Copenhagen, Denmark), the extract was collected using soil moisture cups (pore size 0.15 μm, Rhizons SMS, Rhizosphere Research Products, Wageningen, the Netherlands), and analysed colourimetrically for nitrate (NO_3^-) and ammonium (NH_4^+) on a Seal auto-analyser III (SEAL analytical, Norderstedt, Germany) using hydrazine sulphate and salicylate reagent, respectively.

2.5. Porewater analyses

The pH of all porewater samples was measured as described above. Dissolved inorganic carbon (DIC) content was determined by injecting a known sample volume into a compartment holding 0.4 M H_3PO_4, after which an infra-red gas analyser (Advance Optima IRGA, ABB, Zürich, Switzerland) measured the inorganic carbon (as CO_2) in the gas phase. The concentrations of CO_2 and HCO_3^- were subsequently determined based on the pH equilibrium and a five point calibration curve (0.25–2.5 mM $NaHCO_3$). Concentrations of nitrate (NO_3^-) and ammonium (NH_4^+) were determined colourimetrically on an auto-analyser as described above. Chloride (Cl^-) concentrations were determined colourimetrically on a Seal auto-analyser III system using mercury(II)cyanide as the reagent. Acidified samples (0.1 mL 65 % HNO_3) were analysed for total dissolved elemental content of Ca^{2+}, Mg^{2+}, Fe^{2+}, P and S on the ICP-OES. After removing the vacuum with N_2 gas and equilibrating, concentrations of methane (CH_4) and sulphide (S^{2-}; measured from April 2020 until July 2021) were measured in the headspace of the exetainers by injecting a known volume into a 7890B gas chromatograph (Agilent Technologies, Santa Clara, CA, USA) equipped with a Carbopack BHT100 glass column (2 m, ID 2 mm), flame ionisation (FID) and flame photometric detector (FPD). Concentrations of dissolved organic carbon (DOC) were measured on a TOC-L CPH/CPN analyser (Shimadzu, Kyoto, Japan) after acidification with HCl (2 M, 0.15 mL per 10 mL) to remove DIC. In the text, all concentrations (in μmol/L) and GWLs are presented as mean ± sd.

2.6. Redox

Redox potential (Eh) was measured at 10, 30, 50, 70 and 90 cm depth with a measuring interval of 1 min. Every 30 min an average was calculated and saved on the data loggers. Daily averages were calculated per depth on each probe. All Eh measurements were standardized to pH 5.5 (average porewater pH) using the corresponding porewater pH to allow comparison across locations and determination of Eh ranges. For more details, see Boonman et al. (2024).

2.7. Statistical analyses

To test whether GWLs, Eh, porewater pH and porewater concentrations of DIC, HCO_3^-, NH_4^+, Fe^{2+}, S, P, DOC and CH_4 had different intercepts or patterns over time for SSI and control plots, generalised additive mixed models (GAMM) were used. In these models, a linear term of a generalised model can be replaced by a smooth term to describe non-linear relationships (Wood, 2017). Treatment (SSI or Control) was added as a parametric factor to test for different intercepts. Additionally, to test whether both plots showed different patterns over time, a factor-smooth interaction between day and OFtreatment was added to the model. OFtreatment is the ordered factor of treatment. With ordered factors, the model uses one group within a factor (in this case Control) as a reference and compares this to the other groups (in this case "SSI"). To account for repeated sampling over time, sample ID (label) was included as a random effect. The model used thus was:

$Y \sim$ treatment + s(day, by = OFtreatment) + s(day, replicate, bs = re, m = 1)

where Y is the dependent variable, OFtreatment is the ordered factor used as fixed explanatory variable, s(day, by = OFtreatment) is the smoother term describing the patterns over time relative to the Control and s(day, replicate, bs = 're') is a smoother that fits a random variable to the model to account for repeated sampling at the same location. To determine whether drain distance had an effect on patterns and intercepts within the SSI plot, the following model was used on a subset of the data containing only observations from the SSI plot:

$Y \sim$ distance + s(day, by = OFdistance) + s(day, replicate, bs = re, m = 1),

where distance is the distance from the sampling location (ceramic cup) to the drain, OFdistance is the ordered factor of distance. The s(day, by = OFimpact) thus describes smoothers for the ¼ and ½ drain distances relative to the reference at the drain. s(day, replicate, bs = 're') is a smoother that fits a random variable to the model to account for repeated sampling at the same location.

All models were run separately for each location and each porewater depth (45, 75 and 120 cm depth) using the mcgv package (Wood, 2017) in R (R Core Team, 2022). For Eh, models were run for the summer periods of 2020 and 2021 separately. Model fit was tested using the gam.check function within the mcgv package and by visually inspecting QQ plots, residuals and histograms. Wigglyness (k) was increased when gam.check indicated poor model fit until fit improved. To test whether using a mixed model was justified, a reduced model excluding the random term was compared to the full model using the compareML function in the mcgv package. Graphs were made with ggplot2 (Wickham, 2016), while the redox plot was made with ggplot2 and ggforce package (Pedersen, 2022). Additional functions from R packages lubridate (Grolemund and Wickham, 2011), dplyr (Wickham et al., 2022) and ggpubr (Kassambara, 2022) were also used.

3. Results

3.1. Groundwater levels

The spring and summer of 2020 and 2022 both showed prolonged periods of drought (Fig. 2). During these dry periods, GWLs in the control plots dropped down to 74 ± 9 and 85 ± 10 (ASD), 98 ± 9 and 104 ± 8 (ZEG), 108 ± 19 and 99 ± 14 (ALB), and 83 ± 7 and 89 ± 8 (VLI) cm below ground level in August 2020 and August 2022, respectively. The application of SSI systems reduced this drop in GWLs by raising levels to approximately 31 ± 7 and 32 ± 4 (ASD), 47 ± 5 and 65 ± 14 (ZEG), 38 ± 2 and 38 ± 5 (ALB) and 65 ± 6 and 71 ± 3 cm (VLI) in August 2020 and 2022, respectively. In ALB, the higher GWLs in the SSI plot would also have (partially) resulted from higher ditch water levels, whereas in ZEG, SSI drains were clogged in August 2022, resulting in lower GWLs than during previous summers. In ASD, GWLs measured at the drain or further away from the drains were quite similar. In ZEG, VLI and ALB, GWLs were approximately 10, 20 and 50 cm lower at maximum drain distance compared to those measured at the drain (Fig. 2; Table A-1). In autumn, GWLs increased again in both 2020 and

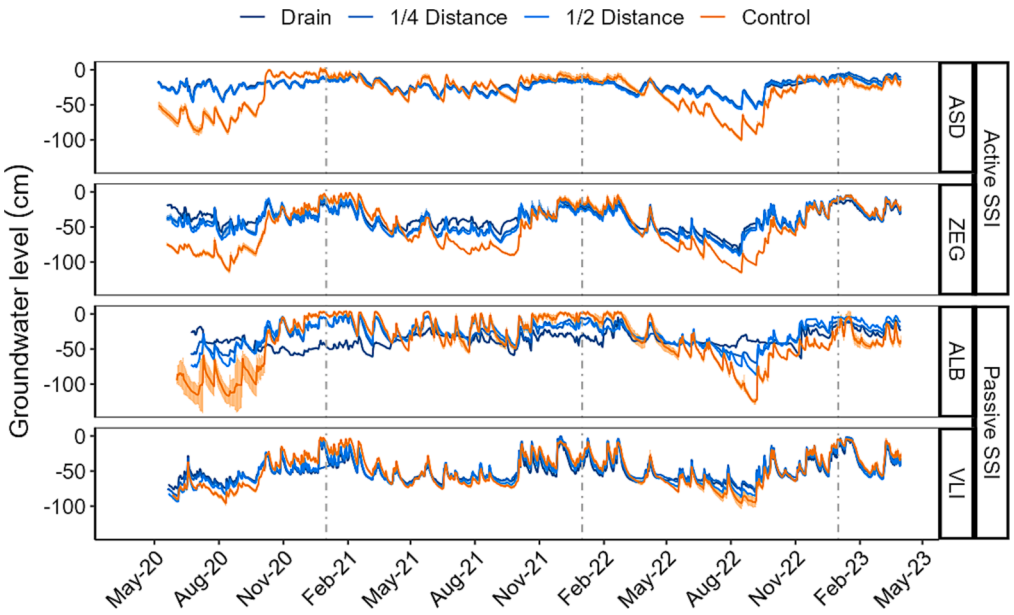

Fig. 2. Mean groundwater level (GWL) in cm below ground level at each of the field locations between April 2020 (in VLI and ZEG, GWL loggers were installed in May 2020) and March 2023. Orange lines represent the GWL of control plots while blue lines represent GWL at SSI-plots, with darker blue close to the drain and lighter blue further away from the drain. Mind different scales on the y-axes. ASD = Assendelft, ZEG = Zegveld, ALB = Aldeboarn and VLI = Vlist. Vertical dotted lines indicate 1 January. Standard deviation is given for control plots (n = 3), whereas on SSI plots, GWL loggers were placed at three distances from the drain.

2022 and remained higher throughout the winter period. During these wetter periods, GWLs were generally 5–15 cm lower on SSI plots compared to control plots. During the wet spring and summer of 2021, GWLs did not drop down as much as in 2020 and 2022. Differences between control and SSI plots were also smaller than during the other summers. Only in ZEG did we see a strong drop in GWLs down to ~ 80 cm below ground level between July and Sept 2021 in the control plot. SSI systems raised these GWLs by 30–40 cm, to approximately 45–55 cm below ground level. Overall, year-round fluctuations in GWL were reduced in SSI plots, although intercepts of SSI and control plots did not differ in VLI (Table A-1).

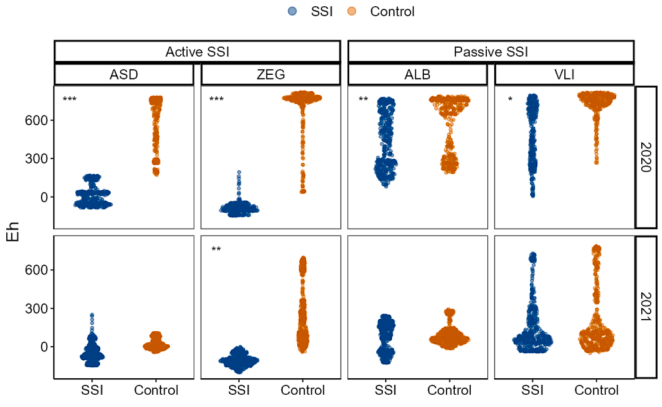

Fig. 3. Redox potential (Eh) measured at 50 cm depth during the spring and summer months (April to August) of 2020 and 2021. Each point represents the daily average Eh (n = 3) on SSI (blue) and Control (orange) plots at Assendelft (ASD), Zegveld (ZEG), Aldeboarn (ALB) and Vlist (VLI). Rather than comparing means, GAMM models were used to determine whether both patterns over time and intercepts differed between SSI and Control plots (see methods for details). Significant differences in intercept between SSI and Control plots are indicated, with * $P < 0.01$, ** $P < 0.05$ and *** $P < 0.001$. Wider scatter indicates a larger number of observations at that Eh value, while a narrow scatter or single observations indicate less frequent Eh values and outliers, respectively.

3.2. Redox

During the summer of 2020, SSI plots generally had lower Eh values than plots without SSI (Fig. 3; Table A-2), especially at locations with active SSI systems (ASD and ZEG). Additionally, at the plots with active SSI systems, the Eh ranges were narrower (−50 to 200 mV) than in their paired control plots (~300 – 800 mV), indicating lower variability. At locations with passive SSI (ALB and VLI), Eh ranges on the SSI and control plots overlapped more, although the control plots still had more observations with higher Eh (>600 mV) than SSI plots. During the wetter summer of 2021, only ZEG still showed differences between Eh measured on SSI and control plots, while the other locations showed no differences (Table A-2), similar to GWL observations discussed in the previous section.

3.3. Porewater composition

3.3.1. Effect of SSI systems on topsoil porewater chemistry during dry summers

Porewater collected at 45 and 75 cm depth in control plots generally showed lower pH (Fig. 4) and DIC (Fig. B-2) concentrations, and higher dissolved-S (Fig. 5), Ca (Fig. B-8) and Mg (Fig. B-9) concentrations than porewater collected in SSI plots at similar depths (Table A-3). These differences were largest during dry periods, such as the spring and summer of 2020 and 2022. Concentrations of dissolved-S doubled in the porewater at 45 and 75 cm depth in control plots in all locations between early spring and late summer 2020. While dissolved-S concentrations were highest in ASD, rising over time from 9 to over 20 mmol/L at 45 cm depth, concentrations also rose sharply from 4 to 10 mmol/L in VLI and ZEG, and from 2 to 4.5 mmol/L in ALB (Fig. 5). Porewater Ca^{2+} and Mg^{2+} concentrations showed the same pattern as dissolved-S. With increasing S, porewater pH dropped at 45 cm depth, with a consistently low pH of 4.5 in ASD in the control plot, whereas VLI and ALB saw decreasing pH during summer months from 5.7 to 5.3 and from 5.0 to 4.4, respectively (Fig. 4). Low pH (4.5 – 5.5) was also observed at 75 cm depth in control plots in ZEG, ALB and VLI. Additionally, spikes in NO_3^- concentration in the porewater were observed in the summers of 2020 and 2021 at 45 cm depth in ASD (up to 200 μmol/L) and ZEG (up to

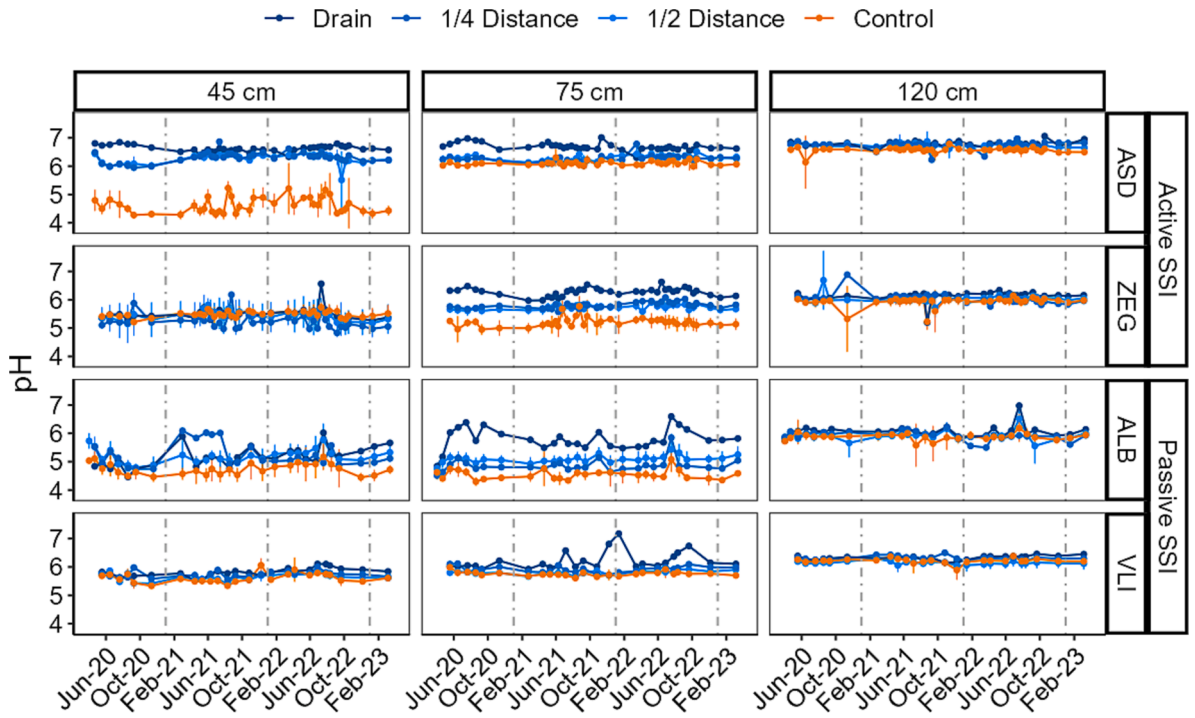

Fig. 4. Mean porewater pH at each of the field locations between April 2020 and March 2023. Orange lines represent the control plots, while blue lines represent SSI plots, with darker blue close to the drain and lighter blue further away from the drain. ASD = Assendelft, ZEG = Zegveld, ALB = Aldeboarn and VLI = Vlist. Vertical dotted lines indicate 1 January. Standard deviation are given for Control plots (n = 5) and ½ drain distance (n = 3).

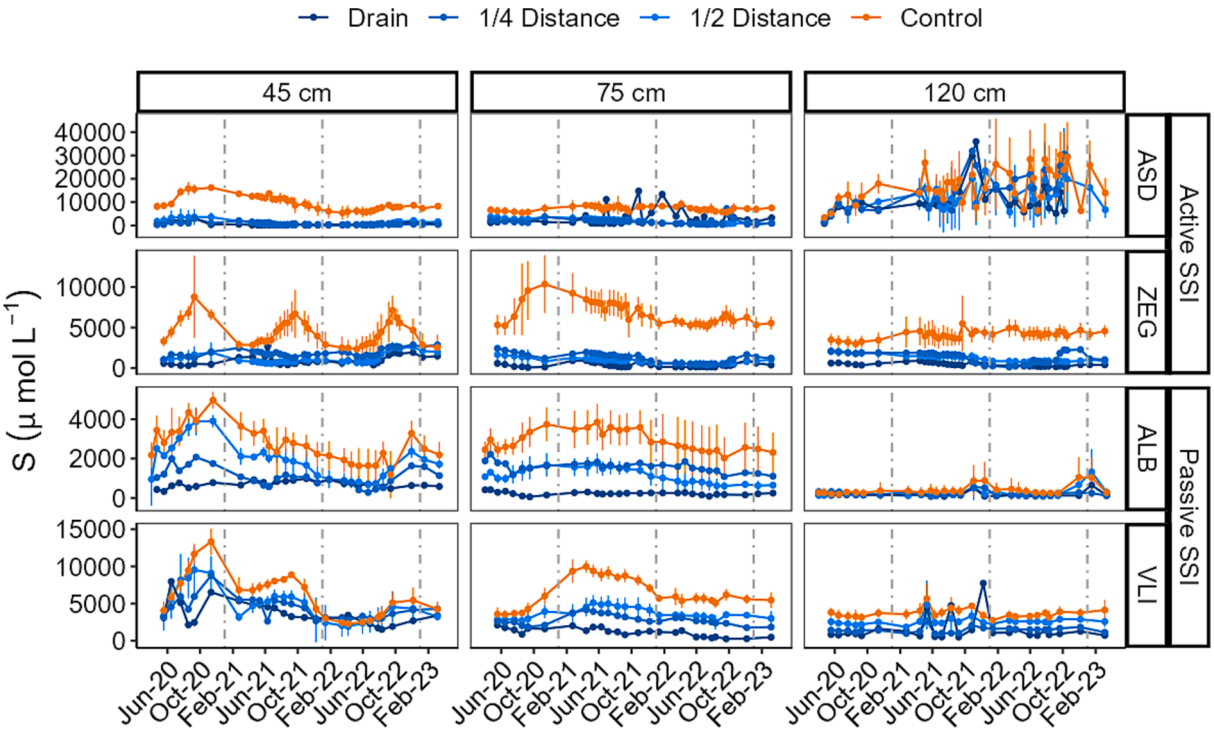

Fig. 5. Mean porewater dissolved sulphur (dissolved-S) concentrations at each of the field locations between April 2020 and March 2023. Orange lines represent the control plots, while blue lines represent SSI plots, with darker blue close to the drain and lighter blue further away from the drain. Mind different scales on the y-axes. ASD = Assendelft, ZEG = Zegveld, ALB = Aldeboarn and VLI = Vlist. Vertical dotted lines indicate 1 January. Standard deviation are given for Control plots (n = 5) and ½ drain distance (n = 3).

3000 μmol/L) in control but not in SSI plots (Fig. B-6; Table A-3).

Porewater Fe^{2+} (Fig. 6), dissolved-P (Fig. B-4), NH_4^+ (Fig. B-5), DOC (Fig. B-3) and CH_4 (Fig. 7) concentrations were generally higher in SSI plots than in control plots (Table A-3), mainly due to concentrations decreasing in the control plots during dry periods (e.g. summers of 2020 and 2022), while remaining stable in the SSI plots. Within the SSI plots,

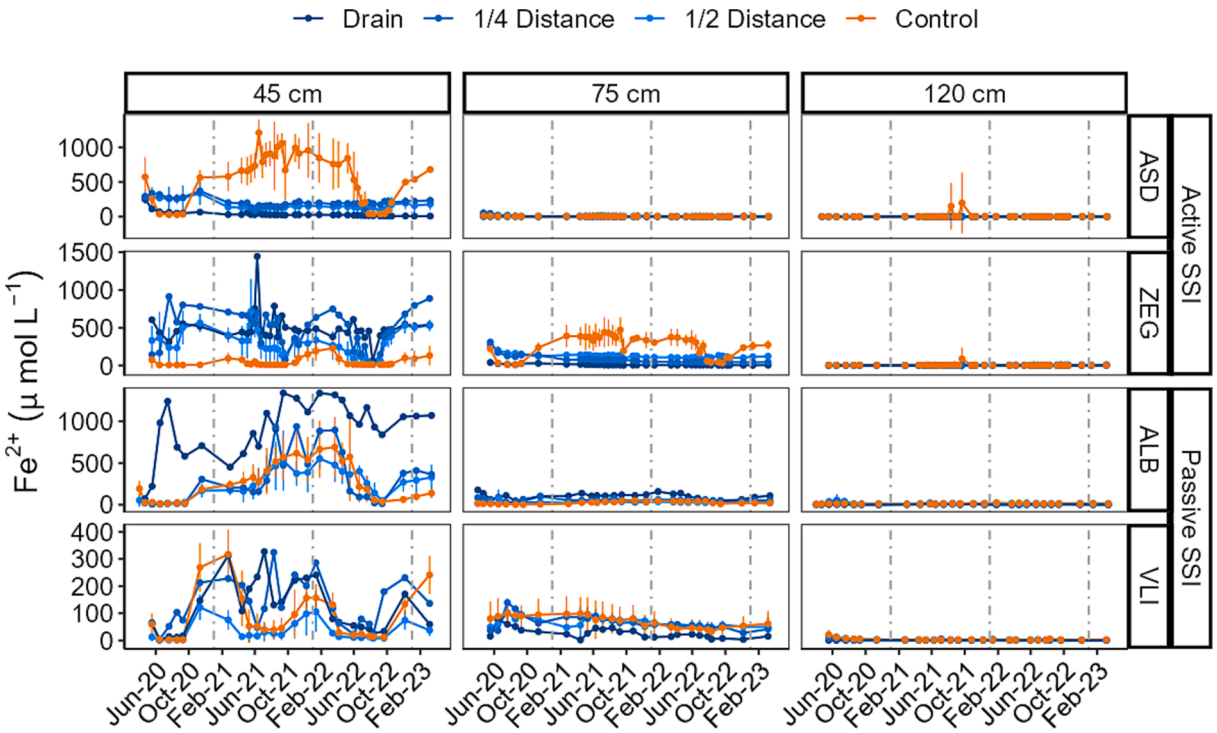

Fig. 6. Mean porewater ferrous iron (Fe^{2+}) concentrations at each of the field locations between April 2020 and March 2023. Orange lines represent the GWL of control parcels, while blue lines represent GWL at SSI plots, with darker blue close to the drain and lighter blue further away from the drain. Mind different scales on the y-axes. ASD = Assendelft, ZEG = Zegveld, ALB = Aldeboarn and VLI = Vlist. Vertical dotted lines indicate 1 January. Standard deviation are given for Control plots (n = 5) and ½ drain distance (n = 3).

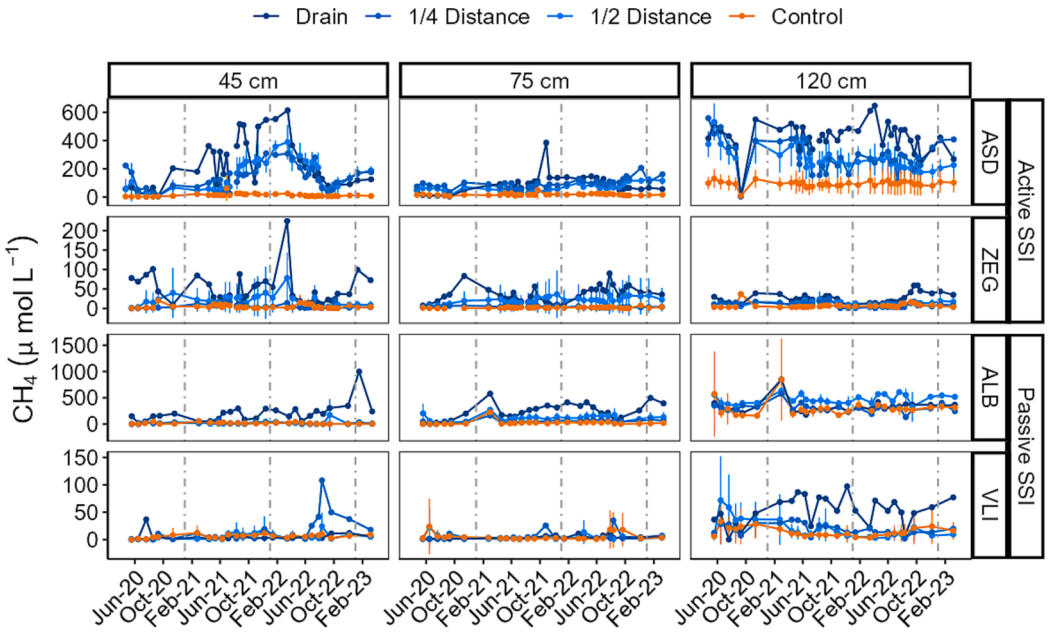

Fig. 7. Mean porewater methane (CH_4) concentrations at each of the field locations between April 2020 and March 2023. Orange lines represent the control plots, while blue lines represent SSI plots, with darker blue close to the drain and lighter blue further away from the drain. Mind different scales on the y-axes. ASD = Assendelft, ZEG = Zegveld, ALB = Aldeboarn and VLI = Vlist. Vertical dotted lines indicate 1 January. Standard deviation are given for Control plots (n = 5) and ½ drain distance (n = 3).

pH and concentrations of Cl^- (Fig. B-10) were generally higher close to the drain (Table A-4). Additionally, in ALB and VLI, concentrations of dissolved-S (Fig. 5), Ca^{2+} (Fig. B-8) and Mg^{2+} (Fig. B-9) collected further away from the drain resembled control plots concentrations (Table A-4).

3.3.2. Effect of SSI systems on topsoil porewater chemistry during winter and wet summers

In autumn and winter, the concentrations of dissolved-S (Fig. 5), Ca^{2+} (Fig. B-8) and Mg^{2+} (Fig. B-9) decreased in the control plots, even though concentrations remained significantly higher than those in SSI

plots during the entire experimental period (Table A-3). Additionally, DIC (Fig. B-2), Fe^{2+} (Fig. 6), P (Fig. B-4) and NH_4^+ (Fig. B-5) concentrations increased in autumn 2020 in the control plots and remained high during the wet summer of 2021. In ASD (45 cm depth) and ZEG (75 cm depth), Fe^{2+} concentrations in the control plot rose to 500–1000 μmol/L, thereby exceeding concentrations in the SSI plot (Fig. 6). Meanwhile, dissolved-P (Fig. B-4), NH_4^+ (Fig. B-5) and DIC (Fig. B-2) concentrations generally remained higher in the SSI plot, even though concentrations increased in the control plots during wet periods. During the spring and summer of 2021, differences between control and SSI plots were smaller than during the same period in 2020 and 2022. While pH remained low in all locations (45 and 75 cm depth; Fig. 4) in the summer of 2021, increases in dissolved-S (Fig. 5), Ca^{2+} (Fig. B-8) and Mg^{2+} (Fig. B-9) were only observed in ZEG and VLI, and final concentrations were lower than during the summer of 2020. While the summer of 2020 saw decreases in Fe^{2+} (Fig. 6), P (Fig. B-4) and NH_4^+ (Fig. B-5) concentrations at the control plot at all locations, these concentrations continued to increase during the summer of 2021 in ASD, ZEG and ALB and only dropped back to lower concentrations in the dry summer of 2022.

3.3.3. *Effect of SSI systems on porewater chemistry in deeper soil layers*

The effects of SSI systems described above were most prominent in soil layers at 45 and 75 cm depth. At 120 cm depth, porewater composition generally showed low Fe^{2+} (Fig. 6) and dissolved-P (Fig. B-4), and higher pH (Fig. 4) and DIC (Fig. B-2). Additionally, concentrations of dissolved CH_4 (Fig. 7) and sulphide (Fig. B-7) were highest in these deeper layers. Even at 120 cm depth, dissolved-S concentrations (Fig. 5; Table A-3) were lower and CH_4 concentrations (Fig. 7; Table A-3) were higher in the SSI plots than in the control plots. Additionally, CH_4 could also be detected in shallower soil layers in SSI plots (Fig. 7). Large differences in CH_4 concentrations existed between locations, with ASD and ALB showing concentrations of up to 600 μmol/L (in SSI plots), while concentrations generally remained below 100 μmol/L in ZEG and VLI. In several locations, CH_4 concentrations were highest close to the drain, especially in shallower soil layers (Fig. 7; Table A-4). Sulphide concentrations were highest in ASD, where S^{2-} was not only detected at 120 cm but also at 75 cm depth (Fig. B-7).

4. Discussion

Our drained agricultural peat soils showed strong fluctuations in GWLs throughout the year, with low levels in summer (60–100 cm below ground level) and high levels in winter (0–20 cm below ground level). These low summer GWLs are caused by a combination of drainage and evapotranspiration, and were therefore less pronounced in relatively wet summers such as 2021. The application of SSI systems significantly raised GWLs during dry periods and reduced seasonal fluctuations. Our long-term dataset showed clear trends in porewater composition that indicated the dominance of anaerobic decomposition processes using alternative electron acceptors, such as NO_3^-, Fe^{3+} and SO_4^{2-}. Since the energy yield of microbial metabolic processes decrease with every subsequent alternative electron acceptor, this switch to anaerobic peat decomposition would slow down peat oxidation. This is in line with the aims of installing SSI systems, as the final goal is to constrain aerobic peat decomposition and thereby reduce land subsidence rates and net greenhouse gas emissions in terms of CO_2 equivalents.

4.1. *Biogeochemical soil processes in drained peat soils*

During periods with low GWLs, aerobic peat decomposition dominates soil processes down to 50–75 cm depth, as was illustrated at our field sites by high Eh values during dry summers and by temporal redox zonation analyses by Boonman et al. (2024). Under these circumstances nutrients (e.g. N, P), organic molecules and other elements are mobilised by peat mineralisation and can be i) used as substrate in microbial soil processes, ii) taken up by the vegetation or iii) washed out to the surrounding surface water. In our control plots, the effects of aerobic decomposition and peat oxidation became apparent through a drop in pH and an increase in dissolved-S concentrations in the porewater. This increase in dissolved-S is especially apparent in the S-rich location of ASD, but even the S-poorer sites such as ALB showed doubling of porewater S-concentrations. During aerobic peat decomposition and oxidation of reduced (iron)sulphur complexes (such as pyrite) in the upper soil layers, protons (H^+) and SO_4^{2-} are produced (Lucassen et al., 2002; Smolders et al., 2006). HCO_3^- in the porewater undergoes protonation to form either H_2CO_3 or CO_2, which can be easily released to the atmosphere through air-filled pore spaces. This explains the lower DIC and HCO_3^- concentrations in control plots during times of low GWLs. Porewater Ca^{2+} and Mg^{2+} concentrations increased, which indicates that acid-buffering through dissolution of carbonate complexes (such as $CaCO_3$ and $CaMg(CO_3)_2$) or cation exchange was taking place (Smolders et al., 2006).

After oxygen, NO_3^- and Mn^{4+} are considered the highest energy-yielding alternative electron acceptors. Since soil Mn concentrations were relatively low, Mn^{4+} is not expected to be an important electron acceptor in these soils. NO_3^-, on the other hand, would be available from fertilisation or peat mineralisation. During peat mineralisation, N becomes available as NH_4^+, which is subsequently nitrified to NO_3^- in the presence of oxygen (Tiemeyer et al., 2007). Regular spikes of high porewater NO_3^- concentrations were observed in the upper soil layers during dry periods, especially in locations rich in dissolved N (ASD and ZEG). Simultaneously, decreasing porewater Fe^{2+} and P concentrations indicate that oxidation of Fe^{2+} into Fe^{3+} was taking place. This Fe^{3+} precipitates as iron(III)(hydr)oxides, which can bind and immobilise P (Lucassen et al., 2005; Smolders et al., 2006). Years of agricultural activity and cyclical oxidation have caused the accumulation of Fe-bound P in drained agricultural peatlands such as our study sites (van Diggelen et al., 2020; Zak et al., 2017).

High GWLs in autumn and winter reduce the intrusion of oxygen into the upper peat layers (Estop-Aragonés et al., 2012), causing reduction processes to become dominant. These processes consume protons and produce HCO_3^-, thereby increasing the pH. Decreasing S concentrations in the porewater of control plots indicate that SO_4^{2-} reduction processes take place, while increases in Fe^{2+} and P concentrations reveal the occurrence of iron reduction and the mobilisation of iron-bound P. During the dry period in 2020, a lot of reduced FeS compounds would have been oxidised, especially in the control plots, after which Fe^{3+} accumulated as poorly soluble iron(III)(hydr)oxides (Lucassen et al., 2005). With increasing GWLs, these iron(III)(hydr)oxides were reduced again, resulting in the continued mobilisation of Fe^{2+} in these soil layers. In ALB and ASD, this mobilisation continued into the spring and summer of 2021, as conditions remained wet and GWLs remained high. The occurrence of such legacy effects reveals interactions between subsequent dry and wet years and thus illustrates the importance of measuring biogeochemical dynamics over several years. During periods with higher GWLs, NH_4^+ concentrations also increased in the control plots at most locations. This could be explained by accumulation of NH_4^+ produced during anaerobic peat decomposition due to lower nitrification rates under anaerobic soil conditions and lower temperatures, possibly combined with the reduced uptake of N by the vegetation.

Deeper soil layers (~120 cm below ground level) remain saturated year-round and therefore show less seasonal fluctuations in porewater composition. In these layers, P and NH_4^+ concentrations are generally high, while Fe^{2+} concentrations are low due to the formation of FeS compounds (Lucassen et al., 2002; Smolders et al., 2006). Additionally, the anaerobic conditions prevalent at 120 cm depth support methanogenesis, which is illustrated by consistently higher CH_4 concentrations than in shallower soil layers.

4.2. Effects of SSI systems on soil biogeochemical processes

Application of SSI systems reduced GWL fluctuations and raised GWLs during dry periods. As a result, zonation of soil redox processes becomes more stable throughout the year. This was confirmed by a recent study by Boonman et al. (2024). In our study, we saw less fluctuation in Eh values in SSI plots and overall lower Eh values during dry periods compared to control plots, indicating that anaerobic processes become more dominant in shallower soil layers. In shallow, iron-rich soil layers, Fe(III)(hydr)oxides are reduced to Fe^{2+}, which lowers the binding capacity of P (Lamers et al., 1998; Smolders et al., 2006). This is illustrated by the higher Fe^{2+} and P concentrations in the porewater of SSI plots compared to control plots during the summers of 2020 and 2022. Additionally, increased availability of aluminium (Al^{3+}) in some locations suggests that P could also have been bound in recalcitrant ionic Al-Fe complexes (sesquisoxides) (Grenon et al., 2021), which are pH- rather than redox-sensitive. Below the shallow oxic layer, year-round reducing conditions ensure that all Fe^{3+} would already have been reduced to Fe^{2+}. As a result, SO_4^{2-} and inorganic C become the dominant electron acceptors, depending on their availability in the different locations. Especially during the wet summer of 2021, dissolved CH_4 concentrations were high in SSI plots, even in the deeper soil layers down to 120 cm depth. This indicates that the effects of infiltration were not limited to the upper soil layers.

P, HCO_3^-, Fe, NH_4^+ and DOC are released during anaerobic decomposition of peat and accumulate in the porewater (Höll et al., 2009; van Diggelen et al., 2020). NH_4^+, for example, accumulates because nitrification is inhibited under anoxic conditions (Paulissen et al., 2005). By supplying a direct connection between anoxic soil layers and the surface water, infiltration systems could speed up the transport of these nutrients and (in)organic carbon during times of drainage, thus possibly negatively affecting surface water quality in the surrounding ditches and canals. Mobilisation of DOC, NH_4^+ and P has been observed in rewetted peat soils, especially in those rich in iron (Emsens et al., 2016; Selle et al., 2019; Zak and Gelbrecht, 2007). Additionally, lateral transport of nutrients and (in)organic carbon could promote the production and emission of greenhouse gases in surrounding ditches and surface waters (Peacock et al., 2021). Aerobic peat decomposition in drained peat meadows and subsequent run-off, on the other hand, is also a strong contributor to nutrient loading of surrounding surface water (van Beek et al., 2007; Vermaat and Hellmann, 2010). Furthermore, SO_4^{2-} produced during soil oxidation can indirectly have a strong negative effect on water quality in the ditches by increasing the mobility of P in ditch sediments (Geurts et al., 2010; Smolders and Roelofs, 1993; van Diggelen et al., 2020). Given the poor state of surface water quality in the Netherlands (van Gaalen, et al., 2020), it would be important to quantify the effect of drainage and application of SSI systems in agricultural peatlands on surface water quality. According to Van Diggelen et al, (2020) wetter conditions in peatlands could both have positive and negative effects on surrounding surface water quality, also depending on the time scale being looked at. Although modelling has been used to estimate the impact of SSI systems on water quality (Hendriks and van den Akker, 2012), field measurements remain scarce.

SSI systems use surface water for infiltration during periods of drought, which can be a source of electron donors (i.e. organic carbon) and electron acceptors (i.e. O_2, NO_3^- and SO_4^{2-}) in deeper, anoxic soil layers. Inlet of more energetically favourable electron acceptors such as oxygen and NO_3^- could stimulate peat decomposition in layers generally dominated by SO_4^{2-} reduction and methanogenesis, which may be amplified due to increases in soil temperature (Boonman et al., 2022). Oxygen concentrations in the drain water were not determined in our study sites, but spikes of NO_3^- concentrations were observed in drains and in deeper soil layers during periods of surface water infiltration at several locations. In a strongly reducing environment, both oxygen and NO_3^- would be used up very quickly, which implies that the effect of the supply of electron acceptors via the infiltration water will mainly be restricted to the soil immediately surrounding SSI drains. Local effects on porewater composition around SSI drains were visible through higher pH and Cl^- concentrations during inlet of surface water. Additionally, CH_4 concentrations were higher around the drain, possibly because wet conditions around SSI drains contained more anaerobic pockets where all other alternative electron acceptors had been used up to allow methanogenesis.

4.3. Active versus passive SSI systems

Locations with active systems showed stronger effects of SSI on GWLs than locations with passive systems. Especially during dry periods, GWLs showed fewer drops and less fluctuation in sites with active rather than passive SSI systems, since surface water is actively pumped into a reservoir, which allows users to set target GWLs (Hoekstra et al., 2020). During dry periods, GWLs still dropped considerably at sites with passive SSI, but not as much as in control sites. The difference between the effects of passive and active SSI systems on GWLs was also reflected in the redox zonation and porewater composition. Findings by Weideveld et al. (2021) and Boonman et al. (2022) on effects of SSI on greenhouse gas emission may also be traced back to differences in efficiency between passive and active SSI. Still, site-specific differences existed in both active and passive sites. In ASD, the active SSI system were installed at a shallower depth and were set to a higher target value than in ZEG. As a result, GWLs were higher, which resulted in stronger effects on biogeochemistry and redox dynamics at 45 cm below ground level than in ZEG. Especially in combination with the high FeS content of the sediment, ASD showed the strongest responses in pH, SO_4^{2-} mobilisation and Fe^{2+} oxidation. Out of the two passive SSI sites, VLI showing smaller differences in GWLs between SSI and control plots than ALB. This could be partially explained by differences in water management, with higher ditch water levels in ALB, ensuring more stable water supply to passive SSI systems during drier periods. Since we studied two locations with active and two with passive SSI, site-specific differences could confound differences in efficiency between these two types of SSI and we should be careful to draw strong conclusions from a limited sample size.

In addition to smaller effects of passive SSI on GWLs and soil processes compared to active SSI systems, these effects were also more localised, with the strongest effects being observed around the drain inlet, indicating the very low lateral water conductivity of these peat soils. At active SSI plots, on the other hand, drain distance had a much smaller effect on the GWLs or porewater composition. This illustrates that pressurised, active infiltration systems were more efficient at raising GWLs during dry periods and maintaining these higher GWLs throughout the parcel, rather than only close to the drain. As a result, these locations showed fewer differences in porewater composition between samples collected at different distances to the drain. In locations with passive SSI systems, GWLs and porewater concentrations of Ca, Fe^{2+}, Mg and S differed considerably between the three drain distances, with GWLs and porewater furthest from the drain resembling the control plot. Since passive SSI systems depend on surface water (ditch water) levels being at least 10 cm higher than GWLs, low surface water levels during drought can reduce the infiltration and thus the efficiency of passive SSI systems. Active SSI systems avoid this by actively pumping ditch water into a reservoir to maintain the target GWL in the parcels. Both types of SSI would increase regional water demand (Querner et al., 2012) and have costs associated with installation and management (Hoekstra et al., 2020; Weideveld et al., 2021).

5. Conclusion and implications

Sub-soil infiltration (SSI) systems are being installed as an emission mitigation measure in agricultural peatland areas to raise average GWLs and reduce GWL fluctuations. With these systems, farmers aim to limit peat decomposition, greenhouse gas emission and soil subsidence, while being able to continue dairy farming on these drained peatlands. This

study shows that SSI systems significantly impact soil processes by shifting dominance from oxidation to reduction processes in shallow soil layers (~50–75 cm depth). When reduction processes are dominant, nutrients and organic carbon accumulate in the sediment porewater. Although these substances, including P, Fe and NH_4^+, may be mobilised to the surrounding surface water via the SSI systems, the reduction in aerobic peat decomposition that is achieved by raising GWLs is expected to reduce nutrient and sulphate leaching to surface waters in the long run. Monitoring of nutrient, carbon and sulphate fluxes to the surface water during wet periods and its dependency on site specific soil properties is highly recommended. This would also help to quantify the effects of infiltrating deeper soil layers with surface water, which can contain oxygen or alternative electron acceptors (such as NO_3^-). Despite some studies showing that SSI systems can have a limited effect on greenhouse gas emission, this study has shown that their application universally reduces seasonal fluctuations in GWLs in drained peat soils with potentially significant effects on peat decomposition rates. This study provides evidence that SSI systems shift soil processes in the upper peat layers from mostly aerobic to predominantly anaerobic, which causes peat decomposition rates to slow down, as decomposition processes with alternative electron acceptors are known to be less efficient. Understanding the full effects of the implementation of (active and passive) SSI systems and other mitigation measures helps to make better informed decisions for the future management of drained peatlands.

CRediT authorship contribution statement

Sarah F. Harpenslager: Conceptualization, Methodology, Formal analysis, Writing – original draft, Visualization. **Gijs van Dijk:** Writing – review & editing, Methodology, Conceptualization. **Jim Boonman:** Writing – review & editing, Formal analysis, Visualization. **Stefan T.J. Weideveld:** Investigation, Writing – review & editing. **Bas P. van de Riet:** Writing – review & editing, Methodology, Conceptualization. **Mariet M. Hefting:** Writing – review & editing, Supervision, Conceptualization. **Alfons J.P. Smolders:** Writing – review & editing, Supervision, Conceptualization.

Declaration of competing interest

The authors declare that they have no known competing financial interests or personal relationships that could have appeared to influence the work reported in this paper.

Data availability

Data will be made available on request.

Acknowledgements

This study was conducted within the Netherlands research programme on Greenhouse gas dynamics in peatlands and organic soils (NOBV), which was financially supported by the Dutch government. This project is an interdisciplinary collaboration between the following Dutch partners: STOWA, Deltares, Radboud University, Utrecht University, Wageningen Environmental Research, Wageningen University, Technical University Delft, Vrije Universiteit Amsterdam and B-WARE Research Centre. We would like to thank all researchers, technicians, laboratory staff, farmers and land owners that have facilitated or contributed to this project.

Appendix A. Supplementary data

Supplementary data to this article can be found online at https://doi.org/10.1016/j.geoderma.2024.116787.

References

Arets, E.J.M.M., Van Der Kolk, J.W.H., Hengeveld, G.M., Lesschen, J.P., Kramer, H., Kuikman, P.J., Schelhaas, N.J., 2021. Greenhouse gas reporting for the LULUCF sector in the Netherlands: Methodological background, update 2021. Statutory Research Tasks Unit for Nature & the Environment.

Best, E.P.H., Jacobs, F.H.H., 1997. The influence of raised water table levels on carbon dioxide and methane production in ditch-dissected peat grasslands in the Netherlands. Ecol. Eng. 8, 129–144. https://doi.org/10.1016/S0925-8574(97)00260-7.

Boonman, J., Hefting, M., van Huissteden, C., van den Berg, M., van Huissteden, J., Erkens, G., Melman, R., van der Velde, Y., 2022. Cutting peatland CO2 emissions with rewetting measures. Biogeosciences 19, 5707–5727. https://doi.org/10.5194/bg-19-5707-2022.

Boonman, J., Harpenslager, S.F., Van Dijk, G., Smolders, A.J.P., Hefting, M.M., Van de Riet, B.P., Van der Velde, Y., 2024. Redox potential is a robust indicator for decomposition processes in drained agricultural peat soils: A valuable tool in monitoring peatland wetting efforts. Geoderma 441. https://doi.org/10.1016/j.geoderma.2023.116728.

Borger, G.J., 1992. Draining — digging — dredging; the creation of a new landscape in the peat areas of the low countries. In: Verhoeven, J.T.A. (Ed.), Fens and Bogs in the Netherlands: Vegetation, History, Nutrient Dynamics and Conservation, Geobotany. Springer, Netherlands, Dordrecht, pp. 131–171. https://doi.org/10.1007/978-94-015-7997-1_4.

Bridgham, S.D., Updegraff, K., Pastor, J., 1998. Carbon, Nitrogen and phosphorus mineralization in northern wetlands. Ecology 79 (5), 1545–1561.

de Jong, A.E.E., Guererro-Cruz, S., van Diggelen, J.M.H., Vaksmaa, A., Lamers, L.P.M., Jetten, M.S.M., Smolders, A.J.P., Rasigraf, O., 2020. Changes in microbial community composition, activity, and greenhouse gas production upon inundation of drained iron-rich peat soils. Soil Biol. Biochem. 149, 107862 https://doi.org/10.1016/j.soilbio.2020.107862.

Dean, J.F., Middelburg, J.J., Röckmann, T., Aerts, R., Blauw, L.G., Egger, M., Jetten, M.S., de Jong, A.E., Meisel, O.H., Rasigraf, O., 2018. Methane feedbacks to the global climate system in a warmer world. Rev. Geophys. 56, 207–250.

Emsens, W.-J., Aggenbach, C.J.S., Schoutens, K., Smolders, A.J.P., Zak, D., van Diggelen, R., 2016. Soil iron content as a predictor of carbon and nutrient mobilization in rewetted fens. PLoS One 11, e0153166.

Erkens, G., van der Meulen, M.J., Middelkoop, H., 2016. Double trouble: subsidence and CO2 respiration due to 1,000 years of Dutch coastal peatlands cultivation. Hydrogeol. J. 24, 551–568. https://doi.org/10.1007/s10040-016-1380-4.

Estop-Aragonés, C., Knorr, K.-H., Blodau, C., 2012. Controls on in situ oxygen and dissolved inorganic carbon dynamics in peats of a temperate fen. J. Geophys. Res. Biogeosciences 117. https://doi.org/10.1029/2011JG001888.

Geurts, J.J., Smolders, A.J., Banach, A.M., van de Graaf, J.P., Roelofs, J.G., Lamers, L.P., 2010. The interaction between decomposition, net N and P mineralization and their mobilization to the surface water in fens. Water Res. 44, 3487–3495.

Grenon, G., Singh, B., De Sena, A., Madramootoo, C.A., von Sperber, C., Goyal, M.K., Zhang, T., 2021. Phosphorus fate, transport and management on subsurface drained agricultural organic soils: a review. Environ. Res. Lett. 16, 013004 https://doi.org/10.1088/1748-9326/abce81.

Grolemund, G., Wickham, H., 2011. Dates and times made easy with lubridate. J. Stat. Softw. 40 (3), 1–25.

Harpenslager, S.F., van Den Elzen, E., Kox, M.A., Smolders, A.J., Ettwig, K.F., Lamers, L.P., 2015. Rewetting former agricultural peatlands: Topsoil removal as a prerequisite to avoid strong nutrient and greenhouse gas emissions. Ecol. Eng. 84, 159–168.

Hendriks, R.F.A., van den Akker, J.J.H., 2012. Effecten van onderwaterdrains op de waterkwaliteit in veenweiden (No. 2354). Alterra.

Hoekstra, J., van Schie, A., van Hardeveld, H.A., 2020. Pressurized drainage can effectively reduce subsidence of peatlands – lessons from polder Spengen, the Netherlands. Proc. Int. Assoc. Hydrol. Sci. 382, 741–746. https://doi.org/10.5194/piahs-382-741-2020.

Höll, B.S., Fiedler, S., Jungkunst, H.F., Kalbitz, K., Freibauer, A., Drösler, M., Stahr, K., 2009. Characteristics of dissolved organic matter following 20years of peatland restoration. Sci. Total Environ. 408, 78–83. https://doi.org/10.1016/j.scitotenv.2009.08.046.

Hoving, I.E., Holshof, G., Hendriks, R.F.A., 2020. Effecten waterbeheersmaatregelen op veenweidebedrijven in Noord Holland. Technische en economische consequenties en effecten op bodemdaling en broeikasgasemissie. (No. 1274). Wageningen Livestock Research.

Joosten, H., Sirin, A., Couwenberg, J., Laine, J., Smith, P., 2016. The role of peatlands in climate regulation. In: Bonn, A., Joosten, H., Evans, M., Stoneman, R., Allott, T. (Eds.), Peatland Restoration and Ecosystem Services: Science, Policy and Practice, Ecological Reviews. Cambridge University Press, Cambridge, pp. 63–76. https://doi.org/10.1017/CBO9781139177788.005.

Kassambara, A., 2022. ggpubr: "ggplot2" Based Publication Ready Plots_. R package version 0.5.0.

Kechavarzi, C., Dawson, Q., Leeds-Harrison, P.B., Szatyłowicz, J., Gnatowski, T., 2007. Water-table management in lowland UK peat soils and its potential impact on CO2 emission. Soil Use Manag. 23, 359–367. https://doi.org/10.1111/j.1475-2743.2007.00125.x.

KNMI, 2023. Jaaroverzicht Neerslag en Verdamping in Nederland (JONV; Yearly overview precipitation and evaporation in the Netherlands) Data from the Royal Dutch Meteorological Institute.

Lamers, L.P., Tomassen, H.B., Roelofs, J.G., 1998. Sulfate-induced eutrophication and phytotoxicity in freshwater wetlands. Environ. Sci. Technol. 32, 199–205.

Leifeld, J., Wüst-Galley, C., Page, S., 2019. Intact and managed peatland soils as a source and sink of GHGs from 1850 to 2100. Nat. Clim. Change 9, 945–947. https://doi.org/10.1038/s41558-019-0615-5.

Lucassen, Smolders, A.J., Roelofs, J.G., 2002. Potential sensitivity of mires to drought, acidification and mobilisation of heavy metals: the sediment S/(Ca+ Mg) ratio as diagnostic tool. Environ. Pollut. 120, 635–646. https://doi.org/10.1016/S0269-7491(02)00190-2.

Lucassen, S., Smolders, A.J., Lamers, L.P.M., Roelofs, J.G.M., 2005. Water table fluctuations and groundwater supply are important in preventing phosphate-eutrophication in sulphate-rich fens: Consequences for wetland restoration. Plant Soil 269, 109–115. https://doi.org/10.1007/s11104-004-0554-3.

Lucassen, E.C.H.E.T., Smolders, A.J.P., Roelofs, J.G.M., 2005. Effects of temporary desiccation on the mobility of phosphorus and metals in sulphur-rich fens: differential responses of sediments and consequences for water table management. Wetl. Ecol. Manag. 13, 135–148. https://doi.org/10.1007/s11273-004-0314-4.

Paulissen, M.P.C.P., Besalú, L.E., de Bruijn, H., van der Ven, P.J.M., Bobbink, R., 2005. Contrasting effects of ammonium enrichment on fen bryophytes. J. Bryol. 27, 109–117. https://doi.org/10.1179/037366805X53022.

Peacock, M., Audet, J., Bastviken, D., Futter, M.N., Gauci, V., Grinham, A., Harrison, J. A., Kent, M.S., Kosten, S., Lovelock, C.E., Veraart, A.J., Evans, C.D., 2021. Global importance of methane emissions from drainage ditches and canals. Environ. Res. Lett. 16, 044010 https://doi.org/10.1088/1748-9326/abeb36.

Pedersen, T., 2022. ggforce: Accelerating "ggplot2". R package version 0.4.1.

Querner, E.P., Jansen, P.C., van den Akker, J.J.H., Kwakernaak, C., 2012. Analysing water level strategies to reduce soil subsidence in Dutch peat meadows. J. Hydrol. 446–447, 59–69. https://doi.org/10.1016/j.jhydrol.2012.04.029.

R Core Team, 2022. R: A language and environment for statistical computing.

Selle, B., Knorr, K., Lischeid, G., 2019. Mobilisation and transport of dissolved organic carbon and iron in peat catchments—Insights from the Lehstenbach stream in Germany using generalised additive models. Hydrol. Process. 33, 3213–3225. doi: 10.1002/hyp.13552.

Smolders, A.J.P., Moonen, M., Zwaga, K., Lucassen, E., Lamers, L.P.M., Roelofs, J.G.M., 2006. Changes in pore water chemistry of desiccating freshwater sediments with different sulphur contents. Geoderma 132, 372–383.

Smolders, A.J.P., Lucassen, E.C.H.E.T., Bobbink, R., Roelofs, J.G.M., Lamers, L.P.M., 2010. How nitrate leaching from agricultural lands provokes phosphate eutrophication in groundwater fed wetlands: the sulphur bridge. Biogeochemistry 98, 1–7. https://doi.org/10.1007/s10533-009-9387-8.

Smolders, A., Roelofs, J.G.M., 1993. Sulphate-mediated iron limitation and eutrophication in aquatic ecosystems. Aquat. Bot. 46, 247–253.

Tanneberger, F., Tegetmeyer, C., Busse, S., Barthelmes, A., et al., 2017. The peatland map of Europe. Mires Peat 1–17. https://doi.org/10.19189/MaP.2016.OMB.264.

Tiemeyer, B., Frings, J., Kahle, P., Köhne, S., Lennartz, B., 2007. A comprehensive study of nutrient losses, soil properties and groundwater concentrations in a degraded peatland used as an intensive meadow – Implications for re-wetting. J. Hydrol. 345, 80–101. https://doi.org/10.1016/j.jhydrol.2007.08.002.

Updegraff, K., Pastor, J., Bridgham, S.D., Johnston, C.A., 1995. Environmental and substrate controls over carbon and nitrogen mineralization in Northern Wetlands. Ecol. Appl. 5, 151–163. https://doi.org/10.2307/1942060.

van Asselen, S., Erkens, G., Stouthamer, E., Woolderink, H.A.G., Geeraert, R.E.E., Hefting, M.M., 2018. The relative contribution of peat compaction and oxidation to subsidence in built-up areas in the Rhine-Meuse delta, The Netherlands. Sci. Total Environ. 636, 177–191. https://doi.org/10.1016/j.scitotenv.2018.04.141.

van Asselen, S., Erkens, G., Jansen, S., Aben, R., Hessel, R., van de Craats, D., 2023. Effects of subsurface water infiltration systems on phreatic groundwater levels in peat meadows.

van Beek, C.L., Droogers, P., van Hardeveld, H.A., van den Eertwegh, G.A.P.H., Velthof, G.L., Oenema, O., 2007. Leaching of Solutes from an Intensively Managed Peat Soil to Surface Water. Water. Air. Soil Pollut. 182, 291–301. https://doi.org/10.1007/s11270-007-9339-7.

Van de Riet, B.P., Hefting, M.M., Verhoeven, J.T.A., 2013. Rewetting drained peat meadows: risks and benefits in terms of nutrient release and greenhouse gas exchange. Water. Air. Soil Pollut. 224, 1–12.

Van den Born, G.J., et al., 2016. Dalende bodems, stijgende kosten (No. 1064). Planbureau voor de Leefomgeving.

van Diggelen, J.M.H., Lamers, L.P.M., Loermans, J.H.T., Rip, W.J., Smolders, A.J.P., 2020. Towards more sustainable hydrological management and land use of drained coastal peatlands – a biogeochemical balancing act. Mires Peat 1–12. https://doi.org/10.19189/MaP.2019.APG.StA.1771.

van Gaalen, F., Osté, L., van Boekel, E., 2020. Nationale analyse waterkwaliteit. Onderdeel van de Delta-aanpak Waterkwaliteit (No. 4002). PBL Planbureau voor de Leefomgeving.

Vermaat, J.E., Hellmann, F., 2010. Covariance in water- and nutrient budgets of Dutch peat polders: what governs nutrient retention? Biogeochemistry 99, 109–126. https://doi.org/10.1007/s10533-009-9395-8.

Vorenhout, M., van der Geest, H.G., Hunting, E.R., 2011. An improved datalogger and novel probes for continuous redox measurements in wetlands. Int. J. Environ. Anal. Chem. 91, 801–810. https://doi.org/10.1080/03067319.2010.535123.

Weideveld, S.T.J., Liu, W., van den Berg, M., Lamers, L.P.M., Fritz, C., 2021. Conventional subsoil irrigation techniques do not lower carbon emissions from drained peat meadows. Biogeosciences 18, 3881–3902. https://doi.org/10.5194/bg-18-3881-2021.

Wickham, H., Francois, R., Henry, L., Müller, K., 2022. dplyr: A Grammar of Data Manipulation_. R package version 1.0.10.

Wickham, H., 2016. ggplot2: Elegant Graphics for Data Analysis.

Wood, S.N., 2017. Generalized Additive Models: An Introduction with R, Second Edition, 2nd ed. Chapman and Hall/CRC, Boca Raton. doi: 10.1201/9781315370279.

Zak, D., Gelbrecht, J., 2007. The mobilisation of phosphorus, organic carbon and ammonium in the initial stage of fen rewetting (a case study from NE Germany). Biogeochemistry 85, 141–151. https://doi.org/10.1007/s10533-007-9122-2.

Zak, D., Meyer, N., Cabezas, A., Gelbrecht, J., Mauersberger, R., Tiemeyer, B., Wagner, C., McInnes, R., 2017. Topsoil removal to minimize internal eutrophication in rewetted peatlands and to protect downstream systems against phosphorus pollution: A case study from NE Germany. Ecol. Eng. 103, 488–496. https://doi.org/10.1016/j.ecoleng.2015.12.030.

Ziegler, R., Wichtmann, W., Abel, S., Kemp, R., Simard, M., Joosten, H., 2021. Wet peatland utilisation for climate protection – an international survey of paludiculture innovation. Clean. Eng. Technol. 5, 100305 https://doi.org/10.1016/j.clet.2021.100305.